SciPost Phys. Proc. 18, 013 (2026)

Complete NLO corrections to $t\bar{t}\gamma$ and $t\bar{t}\gamma\gamma$

Daniel Stremmer

Institute for Theoretical Particle Physics and Cosmology,
RWTH Aachen University, D-52056 Aachen, Germany
Institute for Theoretical Particle Physics,
Karlsruhe Institute of Technology, D-76128 Karlsruhe, Germany

⋆ daniel.stremmer@kit.edu

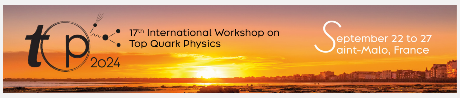

The 17th International Workshop on
Top Quark Physics (TOP2024)
Saint-Malo, France, 22-27 September 2024
doi:10.21468/SciPostPhysProc.18

Abstract

In this contribution we discuss recent progress in associated top-quark pair production with one or two isolated photons, $pp \to t\bar{t}\gamma(\gamma)$. The focus is the simultaneous inclusion of higher-order effects and photon radiation in the production of the top-quark pair and in the decay processes. This allows us to quantify the importance of photon radiation in decay processes and the size of the so-called complete NLO corrections in realistic final states.

Received 2024-12-13
Accepted 2024-12-27
Published 2026-01-29
doi:10.21468/SciPostPhysProc.18.013

1 Introduction

Among the associated production processes of a top-quark pair with a vector boson, $pp \to t\bar{t} + V$ (with $V = \gamma, W^{\pm}, Z$), the $pp \to t\bar{t}\gamma$ process is the dominant one at the LHC and was first observed by the ATLAS collaboration at the center-of-mass energy of $\sqrt{s} = 7$ TeV [1]. This production process inherits many unique challenges with respect to other associated $t\bar{t}$ processes. In particular, a large fraction of photon radiation originates from top-quark decays, which makes the modelling of this process more difficult. In addition, the use of realistic photon isolation conditions leads to further difficulties in theoretical predictions. Finally, the $pp \to t\bar{t}\gamma$ process can be used to probe the $t - \gamma$ coupling.

On the other hand, the $pp \to t\bar{t}\gamma\gamma$ process was not observed yet and is even more affected by these problems due to the additional photon. In addition, this process is part of the irreducible background to the $pp \to t\bar{t}H$ process in the $H \to \gamma\gamma$ decay channel, which was the first single-channel observation of $t\bar{t}H$ [2,3].

In this report we discuss improved theoretical predictions for the two processes $pp \to t\bar{t}\gamma$ and $pp \to t\bar{t}\gamma\gamma$ where we consistently include photon radiation as well as all LO and NLO contributions in the production and the decays of the two top quarks. In addition, we discuss

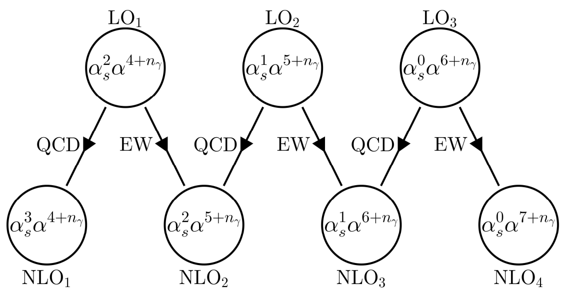

Figure 1: Interplay of LO and NLO contributions for the $pp \to t\bar{t}\gamma(\gamma)$ process with $n_\gamma = 1(2)$. Figure was taken from [5].

the prompt photon distribution for the $pp \to t\bar{t}\gamma\gamma$ process by dividing the full calculation into different resonant contributions based on the origin of the radiated photons in the decay chain. All results shown in this report are taken from Refs. [4, 5], where further information can be found.

2 Process definition and computational setup

In order to study the significance of photon radiation from the decay processes, we include the decays of top quarks and W bosons employing the narrow-width approximation and consider the di-lepton top-quark decay channel. In this case we can split the full calculation of $pp \to t\bar{t}\gamma\gamma$ into three resonant contributions based on the origin of the photons according to

$$\begin{aligned} d\sigma_{\text{Full}} = & \overbrace{d\sigma_{t\bar{t}\gamma\gamma} \times \frac{d\Gamma_t}{\Gamma_t} \times \frac{d\Gamma_{\bar{t}}}{\Gamma_t}}^{\sigma_{\text{Prod.}}} + \overbrace{d\sigma_{t\bar{t}\gamma} \times \left(\frac{d\Gamma_{t\gamma}}{\Gamma_t} \times \frac{d\Gamma_{\bar{t}}}{\Gamma_t} + \frac{d\Gamma_t}{\Gamma_t} \times \frac{d\Gamma_{\bar{t}\gamma}}{\Gamma_t} \right)}^{\sigma_{\text{Mixed}}} \\ & + \underbrace{d\sigma_{t\bar{t}} \times \left(\frac{d\Gamma_{t\gamma\gamma}}{\Gamma_t} \times \frac{d\Gamma_{\bar{t}}}{\Gamma_t} + \frac{d\Gamma_t}{\Gamma_t} \times \frac{d\Gamma_{\bar{t}\gamma\gamma}}{\Gamma_t} + \frac{d\Gamma_{t\gamma}}{\Gamma_t} \times \frac{d\Gamma_{\bar{t}\gamma}}{\Gamma_t} \right)}_{\sigma_{\text{Decay}}}, \end{aligned} \tag{1}$$

where the *Prod.* (*Decay*) contribution refers to the case where both photons are emitted in the production (decay) stage and the *Mixed* contribution contains all cases where we encounter photons simultaneously in the production and decay processes.

The dominant contribution of the $pp \to t\bar{t}\gamma(\gamma)$ process at LO originates from the QCD production of a top-quark pair at $\mathcal{O}(\alpha_s^2\alpha^{4+n_\gamma})$, which we call LO$_1$, where n_γ is the number of photons in the Born process. Additional power suppressed contributions are present at LO at $\mathcal{O}(\alpha_s^1\alpha^{5+n_\gamma})$ (LO$_2$) and $\mathcal{O}(\alpha^{6+n_\gamma})$ (LO$_3$) due to photon initiated subprocesses, the EW production of a top-quark pair and its interference to the QCD production. The sum of all three contributions is simply called LO. The NLO corrections are dominated by the NLO QCD corrections to the LO QCD production (LO$_1$) at $\mathcal{O}(\alpha_s^3\alpha^{4+n_\gamma})$, which is labelled NLO$_1$. The NLO$_{\text{QCD}}$ calculation is then given by the sum of the two contributions, NLO$_{\text{QCD}}$ = LO$_1$ + NLO$_1$, which is then used in the following to quantify the size of the different resonant contributions according to Eq. (1) in the $pp \to t\bar{t}\gamma\gamma$ process and to quantify the importance of the subleading contributions at LO and NLO. As illustrated in Figure 1, we have three additional subleading contributions at NLO due to QCD and EW corrections to different LO contributions. Similar to the LO contributions we label them as NLO$_2$, NLO$_3$ and NLO$_4$. The complete NLO calculation is then given by the sum of all LO and NLO contributions as

$$\text{NLO} = \text{LO}_1 + \text{LO}_2 + \text{LO}_3 + \text{NLO}_1 + \text{NLO}_2 + \text{NLO}_3 + \text{NLO}_4\,. \tag{2}$$

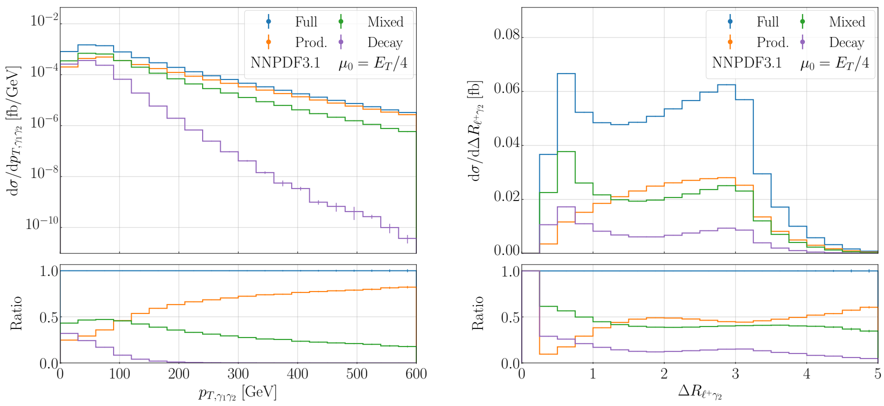

Figure 2: Differential cross-section distributions for the observables $p_{T,\gamma_1\gamma_2}$ and $\Delta R_{\ell^+\gamma_2}$ for the $pp \to t\bar{t}\gamma\gamma + X$ process in the di-lepton decay channel at NLO_{QCD}. Results are presented for the full process and the three resonant contributions *Prod.*, *Mixed* and *Decay*. The lower panels display the ratio to the full calculation. Figures were taken from [4].

In addition, we introduce an approximation, NLO_{prd}, in which we take into account exactly all LO contributions and NLO_1, but we neglect photon radiation and higher-order QCD and EW corrections in the decay processes in all subleading contributions. Thus, NLO_{prd} can be schematically written as

$$\text{NLO}_{\text{prd}} = \text{LO}_1 + \text{LO}_2 + \text{LO}_3 + \text{NLO}_1 + \text{NLO}_{2,\text{prd}} + \text{NLO}_{3,\text{prd}} + \text{NLO}_{4,\text{prd}}\,, \tag{3}$$

where the subscript *prd* indicates that photon radiation and higher-order corrections are taken into account in the production process only. This approximation does not only simplifies the calculation itself a lot, especially the real corrections, but also the matching to parton showers.

The general framework of our calculation is described in detail in Ref. [5] which consists of the matrix element generator RECOLA [6,7] with the program Collier [8] for the calculation of scalar and tensor one-loop integrals, where we have further implemented the random polarisation method [9–11]. In addition, we have implemented a second method for the reduction of one-loop amplitudes using the OPP reduction method [12] with the program CUTTOOLS [13] and the one-loop library [14]. The phase-space integration is performed with PARNI [15] and KALEU [16]. The calculation of the real corrections is carried out with the Nagy-Soper subtraction scheme [11] as implemented in HELAC-DIPOLES [17], which was recently extended for calculations with internal on-shell resonances for arbitrary QCD and QED-like singularities [5].

3 Prompt photon distribution in $pp \to t\bar{t}\gamma\gamma$

The event selection and input parameters used for the following results are described in detail in Refs. [4,5]. First we discuss the prompt photon distribution of the $pp \to t\bar{t}\gamma\gamma$ process in the di-lepton decay channel at NLO_{QCD} and present in Figure 2 the observables $p_{T,\gamma_1\gamma_2}$ and $\Delta R_{\ell^+\gamma_2}$. At the integrated level, the *Prod.* contribution is only 40% of the full calculation. Thus, the cross section is increased by a factor of 2.5 when photon radiation is consistently included in the decays. The observable $p_{T,\gamma_1\gamma_2}$ displays the general behaviour of the three resonant contributions for dimensionful observables. In particular, at small energies the *Mixed* contribution is the dominant one with about 50% of the full calculation while the *Decay* contribution can be as large as the *Prod.* contribution but rapidly decreases in size towards the tail. On the

Table 1: Integrated fiducial cross section for the $pp \to t\bar{t}\gamma + X$ process in the di-lepton top-quark decay channel. Results are presented at LO, NLO, NLO_{QCD} and NLO_{prd} with the corresponding scale uncertainties and for the individual LO and NLO contributions. Table was taken from [5].

		σ_i [fb]	Ratio to LO_1
LO_1	$\mathcal{O}(\alpha_s^2\alpha^5)$	$55.604(8)^{+31.4\%}_{-22.3\%}$	1.00
LO_2	$\mathcal{O}(\alpha_s^1\alpha^6)$	$0.18775(5)^{+20.1\%}_{-15.4\%}$	+0.34%
LO_3	$\mathcal{O}(\alpha_s^0\alpha^7)$	$0.26970(4)^{+14.3\%}_{-16.9\%}$	+0.49%
NLO_1	$\mathcal{O}(\alpha_s^3\alpha^5)$	+3.44(5)	+6.19%
NLO_2	$\mathcal{O}(\alpha_s^2\alpha^6)$	−0.1553(9)	−0.28%
NLO_3	$\mathcal{O}(\alpha_s^1\alpha^7)$	+0.2339(3)	+0.42%
NLO_4	$\mathcal{O}(\alpha_s^0\alpha^8)$	+0.001595(8)	+0.003%
LO		$56.061(8)^{+31.2\%}_{-22.1\%}$	1.0082
NLO_{QCD}		$59.05(5)^{+1.6\%}_{-5.9\%}$	1.0620
NLO_{prd}		$59.08(5)^{+1.5\%}_{-5.9\%}$	1.0626
NLO		$59.59(5)^{+1.6\%}_{-5.9\%}$	1.0717

other hand, the *Prod.* contribution increases towards the tail and becomes the most dominant one with about 80%, while the *Mixed* contribution is still non-negligible with about 20%. The importance of photon radiation in the decays is even more pronounced for angular distributions such as $\Delta R_{\ell^+\gamma_2}$, where we find that the three resonant contributions have different peak structures. In particular, all three contributions are enhanced in the back-to-back region at $\Delta R_{\ell^+\gamma_2} \approx 3$, while the *Mixed* and *Decay* contributions have an additional peak at small angular separations, due to photon radiation in the decay processes, which is completely absent in the *Prod.* contribution.

4 Complete NLO corrections

In the following we concentrate on the $pp \to t\bar{t}\gamma$ process, but the conclusions are the same for $pp \to t\bar{t}\gamma\gamma$. The results of the LO, NLO_{QCD}, NLO and NLO_{prd} calculations at the integrated level with the corresponding scale uncertainties as well as the individual (subleading) LO_i and NLO_i contributions are shown in Table 1. The LO_1 and NLO_1 contributions are the dominant ones at LO and NLO, respectively, while the subleading contributions are individually below 1%. Thus, the NLO_{QCD} calculation is completely sufficient to accurately describe this process at the integrated level and only differs by about 1% with the complete NLO calculation, while the corresponding scale uncertainties are about 6%.

In Figure 3 we present the differential results for the complete NLO calculation in comparison to the LO, NLO_{QCD} and NLO_{prd} calculations for the two observables p_{T,γ_1} and p_{T,b_1b_2}. The lower panels display the ratios NLO_{QCD} over LO, NLO over NLO_{QCD} and the subleading (N)LO contributions over LO_1. We find that the largest subleading effects originate from the NLO_2 contribution, due to EW Sudakov logarithms, which can be as large as 5% − 10% compared to LO_1 in the high-energy tails. This leads to a reduction of about 5% of NLO with respect to NLO_{QCD} for p_{T,γ_1}. On the other hand, both calculations are basically identical for p_{T,b_1b_2} because of accidental cancellations between NLO_2 and NLO_3. The latter contribution is enhanced in the tail due to additional QCD radiation, where a similar pattern can already be found for the NLO_{QCD} calculation due to large real corrections in NLO_1. The differences be-

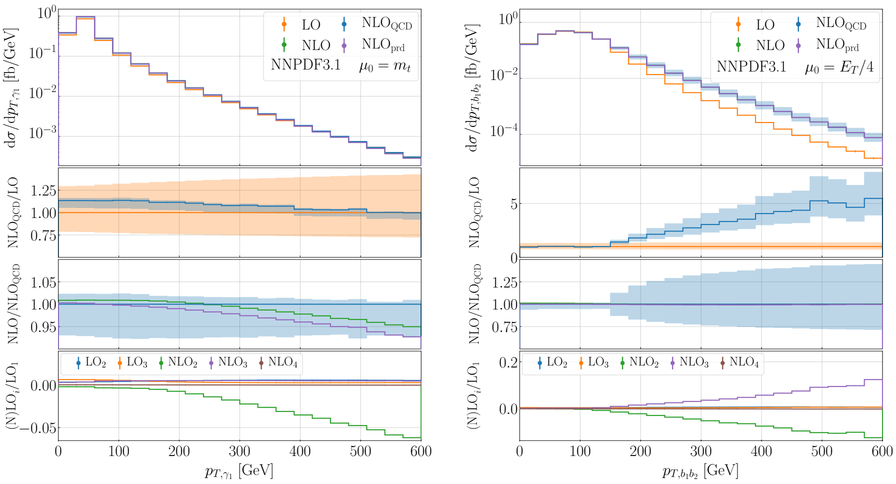

Figure 3: Differential cross-section distributions for the observables p_{T,γ_1} and p_{T,b_1b_2} for the $pp \to t\bar{t}\gamma + X$ process in the di-lepton decay channel. Results are shown at LO, NLO, NLO_{QCD} and NLO_{prd}. The second panels display the ratio of NLO_{QCD} with respect to LO with the corresponding scale uncertainties. The ratio NLO over NLO_{QCD} is shown in the third panels and the ratios of subleading LO and NLO contributions compared to LO_1 are given in the lower panels. Figures were taken from [5].

tween NLO_{prd} and NLO are at most 2% and thus significantly smaller than the corresponding scale uncertainties of about 8% in this case.

5 Conclusion

In this report we have presented the prompt photon distribution in the $pp \to t\bar{t}\gamma\gamma$ process in the dilepton decay channel at NLO QCD, where we have demonstrated that the inclusion of photon radiation is crucial for a precise description, since the *Prod.* contribution is only 40% of the full calculation at the integrated level. At the differential level, the situation is even more pronounced at small energies or for angular distributions such as $\Delta R_{\ell^+\gamma_2}$. On the other hand, the *Prod.* contribution dominates in high-energy tails, but the *Mixed* contribution remains non-negligible with about 20%.

In the second part of this contribution we discussed the calculation of subleading LO and NLO contributions for the $pp \to t\bar{t}\gamma(\gamma)$ process in the dilpeton decay channel. We have found that all subleading effects are negligible small at the integrated level and in sum amounts to 1% with respect to the NLO_{QCD} calculation. The scale uncertainties are about 6% and therefore significantly larger. On the other hand, the subleading contribution NLO_2 is enhanced in high-energy tails of dimensionful observables due to EW Sudakov logarithms and can lead to a reduction of NLO_{QCD} by up to 5%−10%. In addition, we have found accidental cancellations between NLO_2 and NLO_3, where the latter contribution is enhanced in the high-energy regime due to large real QCD corrections. Thus, the two contributions should only be considered together.

Acknowledgments

Funding information This work was supported by the Deutsche Forschungsgemeinschaft (DFG) under grant 396021762 – TRR 257: *P3H - Particle Physics Phenomenology after the Higgs Discovery*.

References

[1] G. Aad et al., *Observation of top-quark pair production in association with a photon and measurement of the $t\bar{t}\gamma$ production cross section in pp collisions at $\sqrt{s} = 7$ TeV using the ATLAS detector*, Phys. Rev. D **91**, 072007 (2015), doi:10.1103/PhysRevD.91.072007.

[2] G. Aad et al., *CP properties of Higgs boson interactions with top quarks in the $t\bar{t}H$ and tH processes using $H \to \gamma\gamma$ with the ATLAS detector*, Phys. Rev. Lett. **125**, 061802 (2020), doi:10.1103/PhysRevLett.125.061802.

[3] A. M. Sirunyan et al., *Measurements of $t\bar{t}H$ production and the CP structure of the Yukawa interaction between the Higgs boson and top quark in the diphoton decay channel*, Phys. Rev. Lett. **125**, 061801 (2020), doi:10.1103/PhysRevLett.125.061801.

[4] D. Stremmer and M. Worek, *Associated production of a top-quark pair with two isolated photons at the LHC through NLO in QCD*, J. High Energy Phys. **08**, 179 (2023), doi:10.1007/JHEP08(2023)179.

[5] D. Stremmer and M. Worek, *Complete NLO corrections to top-quark pair production with isolated photons*, J. High Energy Phys. **07**, 091 (2024), doi:10.1007/JHEP07(2024)091.

[6] S. Actis, A. Denner, L. Hofer, J.-N. Lang, A. Scharf and S. Uccirati, *RECOLA – REcursive computation of one-loop amplitudes*, Comput. Phys. Commun. **214**, 140 (2017), doi:10.1016/j.cpc.2017.01.004.

[7] S. Actis, A. Denner, L. Hofer, A. Scharf and S. Uccirati, *Recursive generation of one-loop amplitudes in the Standard Model*, J. High Energy Phys. **04**, 037 (2013), doi:10.1007/JHEP04(2013)037.

[8] A. Denner, S. Dittmaier and L. Hofer, *Collier: A Fortran-based complex one-loop library in extended regularizations*, Comput. Phys. Commun. **212**, 220 (2017), doi:10.1016/j.cpc.2016.10.013.

[9] P. Draggiotis, R. H. P. Kleiss and C. G. Papadopoulos, *On the computation of multigluon amplitudes*, Phys. Lett. B **439**, 157 (1998), doi:10.1016/S0370-2693(98)01015-6.

[10] P. D. Draggiotis, R. H. P. Kleiss and C. G. Papadopoulos, *Multi-jet production in hadron collisions*, Eur. Phys. J. C **24**, 447 (2002), doi:10.1007/s10052-002-0955-5.

[11] G. Bevilacqua, M. Czakon, M. Kubocz and M. Worek, *Complete Nagy-Soper subtraction for next-to-leading order calculations in QCD*, J. High Energy Phys. **10**, 204 (2013), doi:10.1007/JHEP10(2013)204.

[12] G. Ossola, C. G. Papadopoulos and R. Pittau, *Reducing full one-loop amplitudes to scalar integrals at the integrand level*, Nucl. Phys. B **763**, 147 (2007), doi:10.1016/j.nuclphysb.2006.11.012.

[13] G. Ossola, C. G. Papadopoulos and R. Pittau, *CutTools: A program implementing the OPP reduction method to compute one-loop amplitudes*, J. High Energy Phys. **03**, 042 (2008), doi:10.1088/1126-6708/2008/03/042.

[14] A. van Hameren, *OneLOop: For the evaluation of one-loop scalar functions*, Comput. Phys. Commun. **182**, 2427 (2011), doi:10.1016/j.cpc.2011.06.011.

[15] A. van Hameren, *PARNI for importance sampling and density estimation*, Acta Phys. Pol. B **40**, 259 (2009).

[16] A. van Hameren, *Kaleu: A general-purpose parton-level phase space generator*, (arXiv preprint) doi:10.48550/arXiv.1003.4953.

[17] M. Czakon, C. G. Papadopoulos and M. Worek, *Polarizing the dipoles*, J. High Energy Phys. **08**, 085 (2009), doi:10.1088/1126-6708/2009/08/085.